Chapter 1
Introduction: Overview of DNA Origami as Biomaterials and Application

1.1 Introduction

Recently, DNA based materials in nanotechnology have been gaining extreme attentions of DNA technologists as well as researchers in other related biosciences. Taking advantages of specific bonding of DNA base pairs and also the biological functions of DNA strands, DNA nanotechnology employ DNA molecules as building blocks to construct programmed nanostructures in various nanometer-scaled sizes and multiple dimensions. The DNA nanotechnology is pioneered by Ned Seeman, who created the geometrical DNA motifs from basic small components to complicated structures, which further promoted the specific concept of structural DNA nanotechnology [1, 2]. The precisely designed and assembled DNA nanostructures can be functionalized with various kinds of molecules and then be applied in molecular mechanics, in synthetic chemistry and also in biological analysis by cooperating with biological methods, and it continues to develop in response to advancing technique demands [3–5].

"DNA origami", a new advent programmed method, allows for folding DNA strands into almost any desired shape and in precisely controlled size [6]. This advanced approach, which is based on well-established DNA nanotechnology, exhibits specially convenient preparing process and has already applied a lot as the nanoscaffolds for material-orientated functionalization and also for single molecule analysis [3–5]. This chapter firstly gives a common introduction of the basics of DNA origami technique such as the design and the programmed construction. Furthermore, some recent representative advances of DNA origami-based nanostructures as biomaterials are highlighted for the applications in the selective functionalization, single molecule analysis, cell-targeted delivery and also the molecular machine.

Y. Yang, *Artificially Controllable Nanodevices Constructed by DNA Origami Technology*, Springer Theses, DOI 10.1007/978-4-431-55769-2_1

1.2 2D DNA Origami Nanostructures

DNA origami, a method to create two dimensional (2D) DNA nanostructures in ~100 nm size was developed by Rothemund in 2006 [6]. A long single stranded DNA (M13mp18, 7249 bases) is mixed with a series of sequence-complementary strands called staple strands (~200 strands, each ~32-mer) and then annealed from 95 °C to room temperature over 2 h. The predesigned nanostructure will be well formed, as illustrates in Fig. 1.1a. Besides the rectangular-shaped structure, triangles, smiley face and five-pointer star were successfully constructed. The assembled structures can be easily confirmed by atomic force microscopy (AFM), in which even the hybridized DNA duplexes can be clearly observed in high resolution (Fig. 1.1c).

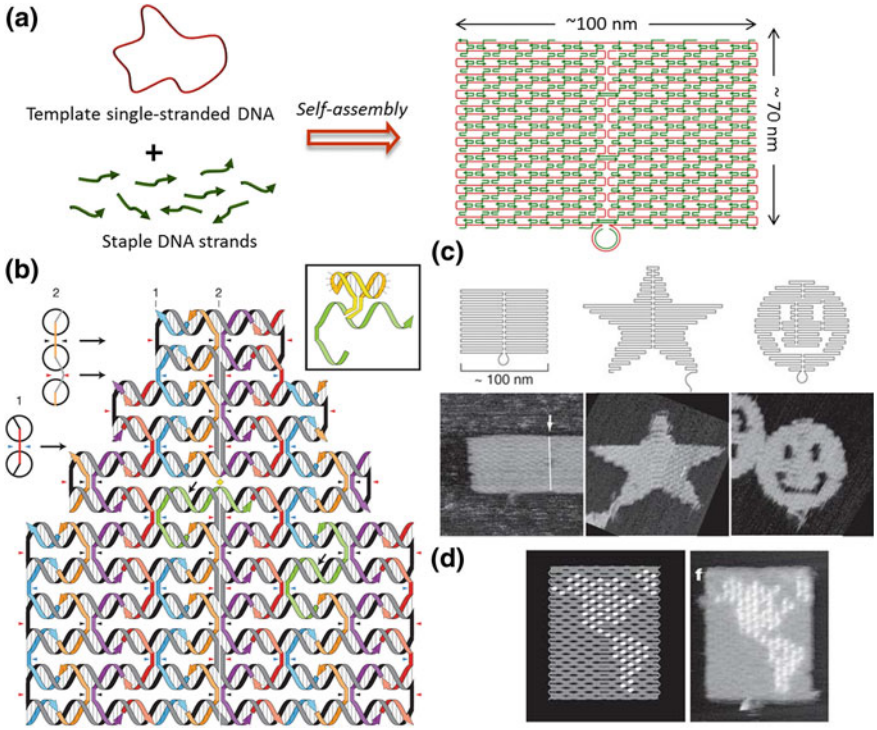

Fig. 1.1 Introduction of DNA origami method. **a** A long single-stranded DNA employed as template assembled with hundreds of staple DNA strands to form a rectangular-shaped nanostructure in a size of ~100 nm × ~70 nm. **b** Detailed design of a DNA origami: the short staple strands connect the adjacent duplexes with crossovers. *Inset* a DNA hairpin structure as a topological marker. **c** Design and AFM images of 2D DNA origami structure in various shapes. **d** Drawing of a hemisphere pattern on a DNA origami with hairpin DNAs (*white dots*) and its corresponding AFM image. Reprinted by permission from Macmillan Publishers Ltd: [Nature] (6), copyright (2006)

The basic design rules are demonstrated in Fig. 1.2b. The adjacent double-stranded DNAs (dsDNAs) are connected by staple strands as crossovers. In this design, the geometry of the double helices involved has three helical rotations for 32 base pairs. Two neighboring crossovers of the central dsDNA in an arrangement of three adjacent dsDNAs should be located at the opposite sites (180° rotated, 0.5 turns). Therefore, the crossovers should be separated by 16 base pairs (1.5 turns). To obtain a planar 2D structure, the multiple staple strands pulling the long strand should be arranged following the same rule. Hundreds of staple strands also afford the possibilities of locating hairpin DNAs as topological markers at desired positions, which are imaged as a dot on AFM images. In principle, the hairpin DNA is placed at a position eight base pairs from the crossover (270° rotation) where the hairpin DNA is located perpendicular to the surface of the origami structure. The distance between neighboring staples strands was calculated around 6 nm, representing that the neighboring hairpin DNAs can be imaged as distinct dots by AFM imaging. As a result, the hairpin DNAs can be employed to constitute various patterns directly on DNA origami surface, such as the map of a hemisphere as shown in Fig. 1.1d. Besides the introduction of the hairpin DNAs into the origami structures, functional molecules and nanoparticles can also integrated into the nanostructures by the modification with staple strands at predetermined positions or by the specific interactions with the specially designed staple strands.

A remarkable property of DNA origami is that each position on the structures possesses one piece of specific sequence information which can be taken as an address no matter the shape variations. Before the advent of DNA origami method, it is quite a challenge to uniformly create nanostructures in a defined size $\sim$100 nm through the assembly of small DNA components. Right now, a big progress is accomplished, which enable no matter the shape design or the size limitation. By using this method, the size of the various geometric DNA origami structures are determined by the template strand: the long single stranded DNA. Various single-stranded DNAs were isolated to serve as the fresh template for the assembly of different nanostructures [7, 8]. A strategy of using DNA tiles (17 × 16 nm) instead of staples has also been developed, which allows size expansion by the introduction of 25–56 DNA tiles [9].

1.3 Programmed Arrangements of Large Sized DNA Nanostructures

The size of single DNA origami structure is constrained around 100 nm because of the length limitations of the single stranded DNA template. To obtain larger-sized structures based on origami method, other techniques are required, which can integrate more complicated functions together.

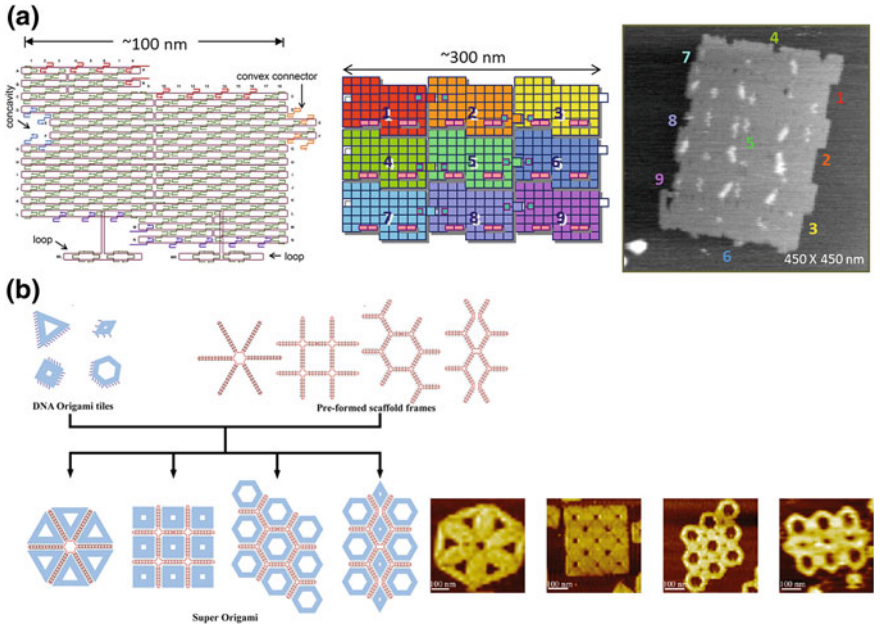

Fig. 1.2 Programmed self-assembly of DNA origami. **a** A DNA origami structure with a concavity and a convex as a "DNA Jigsaw piece" for 2D assembly. A 3 × 3 assembly of nine predesigned origami tiles and its AFM image. Reprinted with permission from (Rajendran, A.; Endo, M.; Katsuda, Y.; Hidaka, K.; Sugiyama, H. *ACS nano* **2010**, *5*, 665–671) Copyright (2010) American Chemical Society. **b** Programmed assembly of "Superorigami" structures by using multiple DNA origami structures scaled up by scaffold frames and their corresponding AFM images. Reprinted with permission from (Nano Letters). Copyright (2011) American Chemical Society

Our group have explored techniques called "Jigsaw pieces" to assemble 2D DNA tiles into larger 2D programmed horizontal or vertical patterns [10, 11]. The assembling tile was designed in a rectangular shape (Fig. 1.2a), in which the tiles can assemble together along the helix axis direction via at the edges. Moreover, specific concave and convex connectors were introduced into the tile to align multiple rectangles precisely with each other. Multiple rectangular tiles can assemble together by both shape and complementary strands which were extended from the staple strands located at the lateral edges of tiles. Nine different tiles were designed and prepared separately. Firstly, three tiles were programmed to assemble together in either vertical or horizontal directions. Secondly, three sets of trimers were finally assembled into a 3 × 3 large structure (300 nm × 240 nm, AFM image in Fig. 1.2a), which is nine-fold larger than single DNA tile.

Rothemund and his co-workers developed a programmed assembly system by regulating the positions of adhesive π-stacking ends for selectively connect rectangular tiles [12]. Besides, Yan's group introduced a template-assisted assembly of different shaped DNA origami monomers into large structures in various patterns

(Fig. 1.2b). The assembling unit assembled with the templates prepared with programmed patterns in a shape complementary rule. As shown in Fig. 1.2b, triangles, rectangles and hexagons were scaled up together in a predesigned manner [13].

The programmed assembly of larger sized nanostructures can be realized by using the above strategies, which can scale up assembling monomers into predesigned patterns and defined size. The extended DNA nanostructures exhibited more address information and provide more opening positions for further functionalization.

Besides using the long single-stranded DNA as scaffold for programmed assembling which requires the helps of hundreds of short "staple" strands, another 'single-stranded tile' (SST) approach [14] was developed by Yin and coworkers. As shown in Fig. 1.3a, a SST motif consists of 4 domains in a total length of 42 nucleotides, which composed of concatenated sticky ends assembled with four

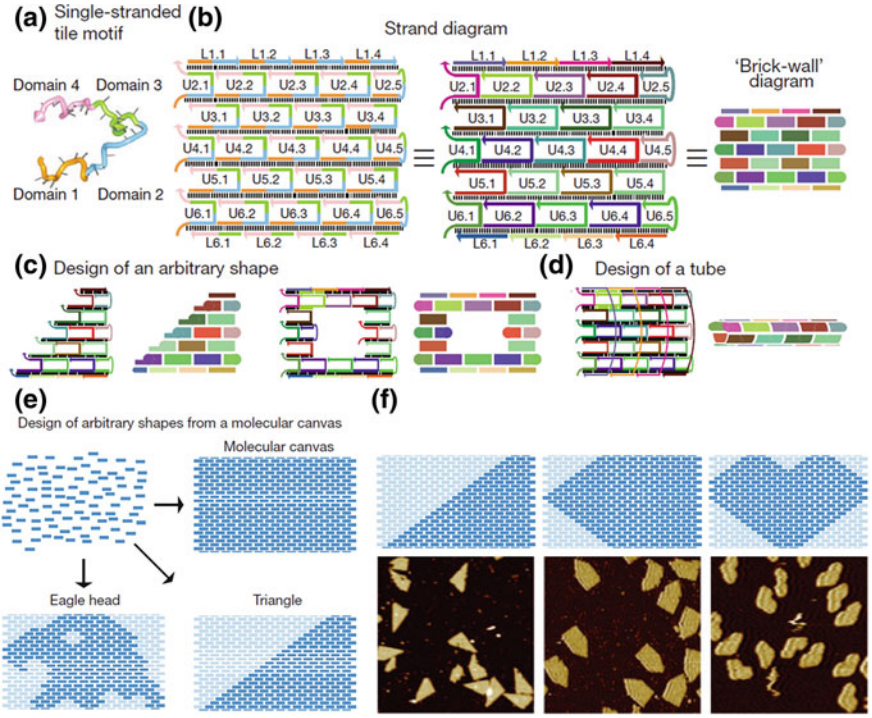

Fig. 1.3 **a** Single-stranded tile motif consisting of four domains in 2 parallel pairs as referred from Ref. [16]. **b** Schematic diagram of rectangular 'brick wall' in 6 helix × 8 helical turn (6H × 8T). Each strand has a unique sequence. **c** An arbitrary shape, triangle (*left*) or rectangular ring (*right*), is formed by selecting proper subset of SST tiles from the groups in (**b**). **d** A tube structure with prescribed width and length. **e** Taken each SST tile as a molecular pixel, molecular canvas or derived eagle head and triangle shaped structured can be designed freely. **f** Simple shapes were designed and constructed using a molecular canvas. Reprinted by permission from Macmillan Publishers Ltd: [Science] (15), copyright (2012)

neighboring strands [15]. A 'brick wall' pattern is formed by arranging a series of distinct SST tiles into lattices (Fig. 1.3b), in which one SST tile can be folded into a 3 nm-by-7 nm tile and associate with four neighboring tiles acting as a pixel. Based on this strategy, any arbitrary shapes of nanostructures using different combinations of SST tiles can be assembled even a tube by connecting half-tiles on the top and bottom boundaries into full tiles (Fig. 1.3c, d). Moreover, a predesigned rectangular lattice can also be viewed as a 'molecular canvas' (shown in Fig. 1.3e) in which each SST tile serves as one 'molecular pixel'. By selecting constituent 'molecular pixels' on the canvas, such as eagle head and triangle (Fig. 1.3e), multiple shapes are formed and constructed, as illustrated in Fig. 1.3f. This SST strategy allows the self-assembly of desired complex structures without the specific scaffold routing design. No matter SST method or conventional DNA origami strategy, both shows that a vast space for developing various approaches for the construction of nucleic acid nanostructures.

1.4 3D DNA Origami Nanostructures

DNA origami nanostructures can be not only extended into larger size in two dimension, but also can be designed and assembled into 3D geometry. Two strategies were developed for the construction of 3D origami structures. One is to bundle neighboring DNA helices by crossovers which is designed according to the structural characteristics of DNA duplex in B-form. Another is to join 2D DNA origami domains into 3D layouts by corresponding interconnection strands. The former method developed by Shih and his coworkers, the relative adjacent DNA helices are joined by crossovers into tubular and multilayered, where the positions of the crossovers can be arranged under the geometrical control (Fig. 1.4a) [16].

A DNA box was constructed by joining up six rectangle origami domains using interconnecting strands (shown in Fig. 1.4b), which was confirmed by cryo-electron microscopy (cryo-EM) as well as AFM [17]. Interestingly, the lid of 3D box can be initiated to open by the addition of complementary strand employing strand displacement strategy. The opening event was monitored by fluorescence resonance energy transfer (FRET) (Fig. 1.4c). Based on similar method, DNA boxes with controlled inside and outside interface were successfully created by regulating the directions of crossovers at the connection edges [18]. A tetrahedral structures was constructed by connecting four aligned triangles, which were pretreated with an M13mp18 scaffold strand without the formation of independent 2D pieces [19].

Our group introduced a series of hollow prism structures containing different numbers of 2D origami pieces [20]. Interestingly, the high-speed AFM imaging captured the opening events of the hollow 3D tube-like structure in second time-scale. Recently, based on SST strategy, Yin's group developed 3D complex structures using short synthetic DNA strands called "DNA bricks" [21]. Hundreds of unique bricks self-assembled into prescribed 3D shapes just like Legos in one-step.

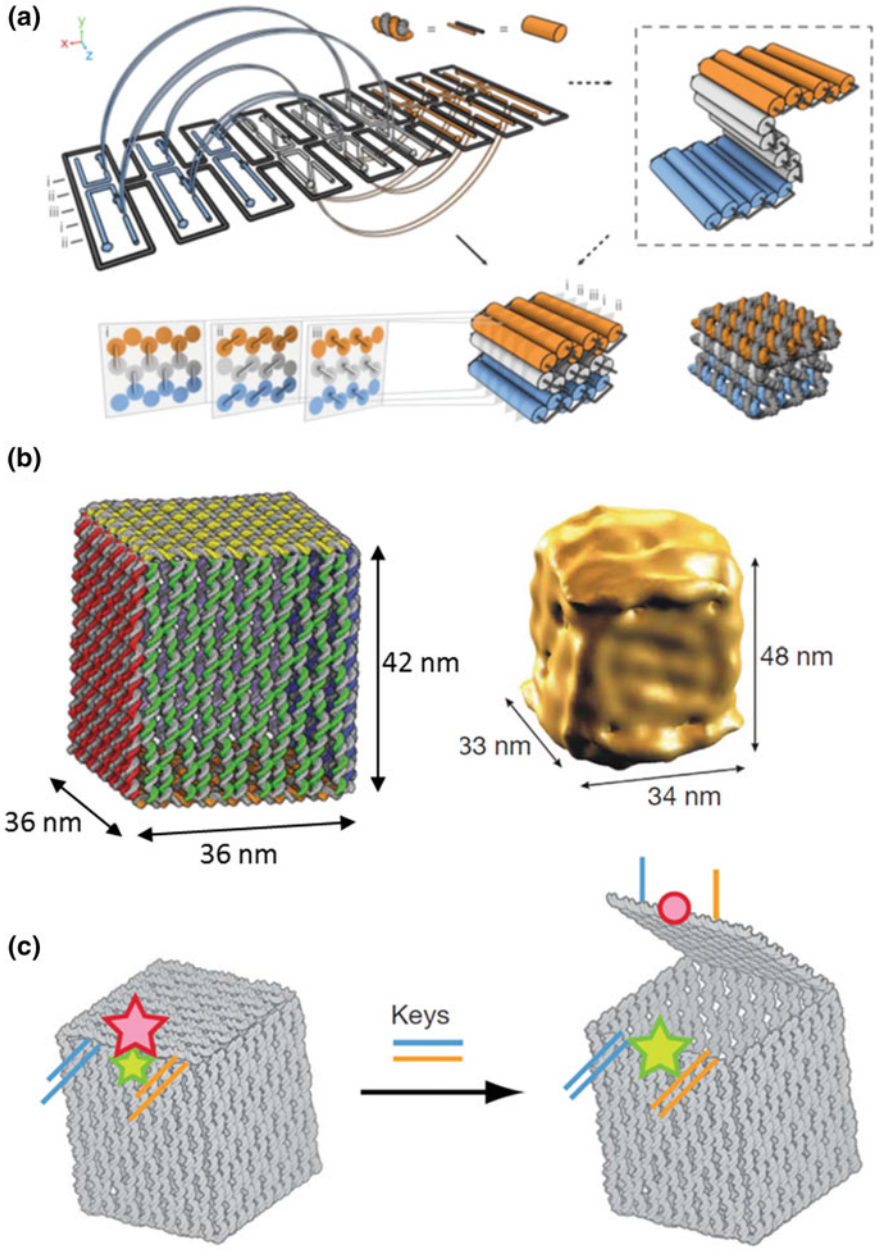

Fig. 1.4 3D DNA box with controlled opening by using strand displacement strategy. **a** 2D pleated structure folded into a 3D multilayered structure using staple strands connecting adjacent layers. Reprinted by permission from Macmillan Publishers Ltd: [Nature] (17), copyright (2009). **b** A 3D DNA box was formed and confirmed by cryo-EM. **c** Controlled opening of the box lid using a selected DNA strand as a key. Lid opening event was monitored by FRET. Reprinted by permission from Macmillan Publishers Ltd: [Nature] (18), copyright (2009)

Besides, a kind of software program: caDNAno was developed, which enable the design of the 3D origami structures directly on computer [22]. More importantly, this program is completely free and open for public. People can freely download it online. And the basic tutorials for starters are also available right now.

1.5 Functionalization of 2D Origami Nanostructures

Each staple strand on DNA origami provides the possibility for addressing and modification with functional groups. In other words, the origami structure affords the desired functionalization at defined positions.

1.5.1 Selective Placements of Functional Groups

Ligands and aptamers are popular particles for the conjugation between DNA strands and proteins, indicating that proteins can selectively attached on the DNA origami by specific recognitions [23–26]. For instance, SNAP-tag and halo-tag were used for the placement of fusion proteins on the DNA origami [27]. Yan's group employed single-stranded DNAs to detect target RNA molecules directly on the DNA origami surface at the single-molecule level by AFM [28]. By employing the streptavidin-biotin labeling, our group designed a five-well nanostructure, which is used for the characterization of alkylation of the sequence selective ligand: pyrrole-imidazole polyamide [29]. The same five-well frame was also applied for the investigation of the Zn-finger protein with target sequence [30]. These studies sufficiently demonstrate that the designed sequence recognition molecules can be used for the placement of proteins on predetermined positions on DNA origami. It is also shown that the AFM imaging can be used to directly confirm functionalization in single molecule level.

1.5.2 Single-Molecule Chemical Reaction

Not only the biomolecules, small organic molecules for specific chemical reactions can be performed and imaged at the local positions of DNA origami by using AFM at single molecule level. Chemical reactions: reductive cleavage of disulfide bonds and oxidative cleavage of olefin by single oxygen were carried out on the DNA origami surface [31]. Besides, amide bond formation and click reactions were also performed on the DNA origami scaffold. Reactive groups: azido, amino and alkyne groups conjugated with staple strands were located at different positions of DNA origami. Three coupling reactions were successively carried out using the

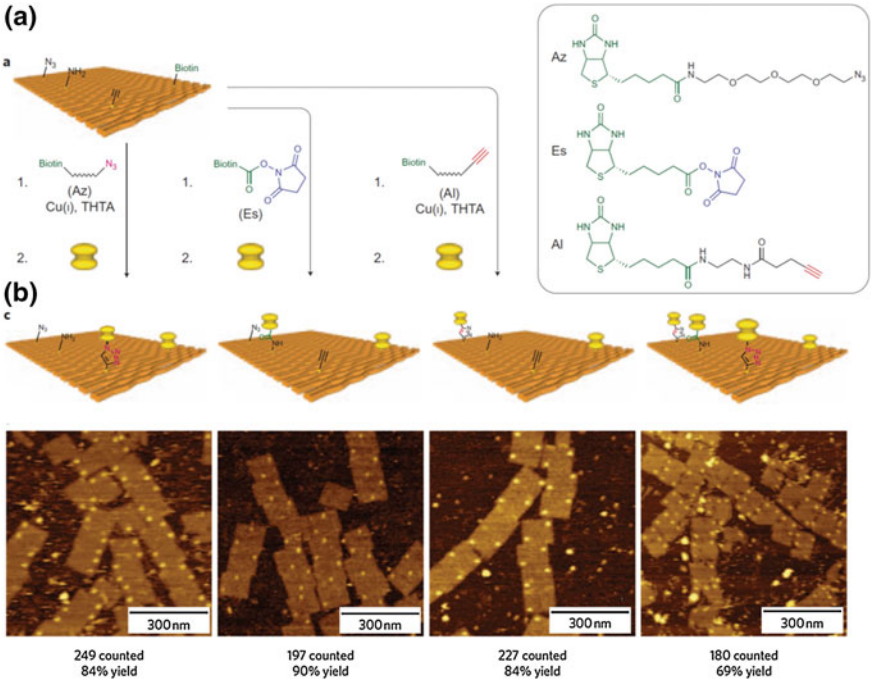

Fig. 1.5 Single chemical reaction on DNA origami. **a** Three active groups: azido, amino and alkyne groups were selected and incorporated together into one single DNA tile by modification with staple strands. The coupling reactions of functional groups attached by biotin were carried out on DNA tile, which were visualized by the specific binding of streptavidin-biotin. **b** AFM images of three reactions performed at different positions. Reprinted by permission from Macmillan Publishers Ltd: [Nature Nanotechnology] (32), copyright (2010)

biotin-attached functional groups (Fig. 1.5). Both of the bond cleavage and the bond formation were characterized by employing streptavidin binding and confirmed by AFM imaging. These chemical reactions all proceeded quantitatively on the defined positions of the DNA origami in high yield.

1.5.3 Selective Modifications with Nanomaterial

Other kinds of nanomaterials can also be integrated into the DNA nanostructures. Gold nanoparticles (AuNPs) coupled with staple strands were selectively placed on DNA origami [32, 33]. The AuNPs can also be encapsulated into a DNA origami cage with addressable and spatial control [34]. Alternatively, thiol-group tethered staple strands can be used to accumulate the AuNPs into DNA origami at predesigned positions in various patterns [35, 36]. Two DNA-modified carbon

nanotubes were arranged into both sides of DNA origami in a cross junction fashion [37]. The position-controlled DNA nanotubes were applied to create a nanodevice, which showed field-effect transistor-like behavior.

1.6 Applications to Single Molecule Analysis

1.6.1 Control of DNA Methylation and DNA Repair in the DNA Nanospace

Nanometer-sized DNA origami can be clearly visualized by AFM as well as the functionalized molecule, indicating that DNA origami structures might be applied as scaffolds for the investigation of interactions between target molecules such as the DNA-enzymatic reactions. DNA-targeted enzymes often require bending specific DNA strands to facilitate the reaction. The dsDNA will be bended by 55–59° during the methyl-transfer reaction by DNA methylation enzyme *Eco*RI methyltransferase (M.*Eco*RI) [38]. To examine the DNA structural effect on the methylation reaction, our group designed a 2D DNA frame containing four connection sites at the inner side (Fig. 1.6a). Two dsDNAs in different lengths: a tense 64-m dsDNA and a relaxed 74-m dsDNA were assembled with the DNA frame (Fig. 1.6b). High-speed AFM was used to analyze the dynamic enzymatic-DNA

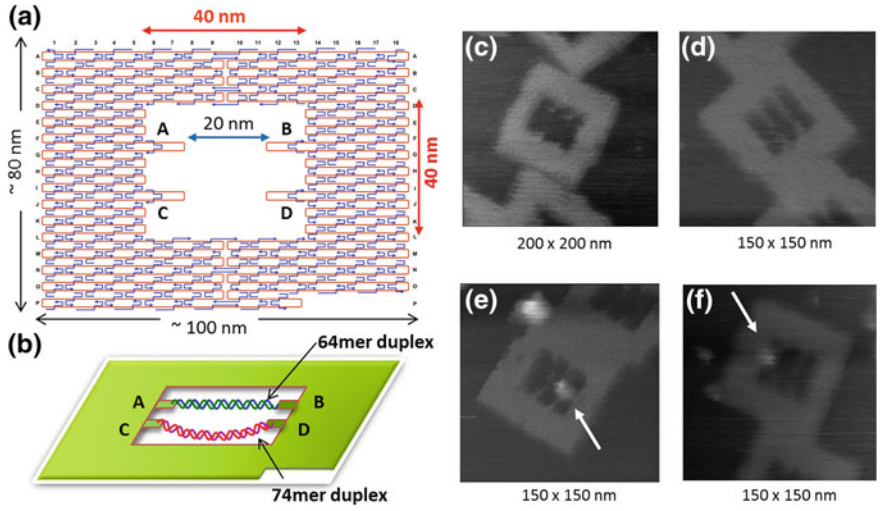

Fig. 1.6 Control of DNA methylation reaction on a DNA frame. **a** Design of the DNA frame containing four connection sites in the inner cavity. **b** Two dsDNAs in different length: AB = tensed 64-m dsDNA and CD = relaxed 74-m dsDNA carrying recognition sequence for M. *EcoRI*, were incorporated into the frame. AFM image of empty DNA frame (**c**), two dsDNA cooperated DNA frame (**d**), and M. *EcoRI* bound to dsDNA of AB (**e**) and CD (**f**), respectively. Reprinted with permission from (Endo, M.; Katsuda, Y.; Hidaka, K.; Sugiyama, H. *J. Am. Chem. Soc.* **2010**, *132*, 1592-1597.). Copyright (2010) American Chemical Society

interaction directly on mica surface. The obtained AFM images revealed that methylation reaction of M. *EcoRI* preferred to occur in the relaxed 74-m dsDNA rather than in the 64-m dsDNA [39]. The results confirmed that the structural flexibility of bending dsDNA is important for the methyl-transfer reaction with M. *EcoRI*.

The same DNA frame was also applied for the analysis of DNA repair reactions and directly visualized by high-speed AFM. DNA base excision repair enzymes: 8-oxoguanine glycosylase [40] and T4 pyrimidinebdimer glycosylase [41] were incorporated into the DNA frame containing various dsDNAs with a damaged base [42]. The DNA repair reactions were examined on the DNA frame in single molecule level. The relaxed 74-m dsDNA trapped the DNA with the cleavage by $NaBH_4$ and exhibited higher cleavage efficiency than 64-m dsDNA. Then the dynamic movements of the enzymes on dsDNA in DNA frame were also directly observed by using high-speed AFM.

DNA origami exhibited as excellent scaffold to integrate with functional molecules for single molecule analysis and the dynamic interactions of active molecules can be directly visualized in the designed nanoscale space by using high-speed AFM imaging.

1.6.2 Visualization of DNA Structural Changes

Not only the DNA-enzymatic interactions can be visualized, but also the structural interaction between DNA strands can be directly observed on DNA origami structures. The reversible G-quadruplex formation and disruption was manipulated on a single DNA frame by using potassium as stimuli [43].

Based on the same frame structure, two G-rich fragments were introduced into the central positions of two dsDNA (both 64-m) separately: three-G-tracts were located in the upper dsDNA whereas the lower dsDNA contained a single G-tract [44] (Fig. 1.7). After the addition of KCl, the two dsDNA were associated together in an X-shape because of the formation of G-quadruplex structure. AFM imaging was employed for the confirmation of the structural changes between two dsDNAs and the yield of the association efficiency was evaluated manually. Furthermore, the real-time dynamic structural changes indicating the formation and disruption of interstrand G-quadruplex were directly observed in different observation buffers with/without K^+ by high-speed AFM. This was the first report of the real-time direct observation of DNA structural changes in limited nano-space. This method can be applied for the analysis of various kinds of nucleic acid-related structural changes in single molecule level.

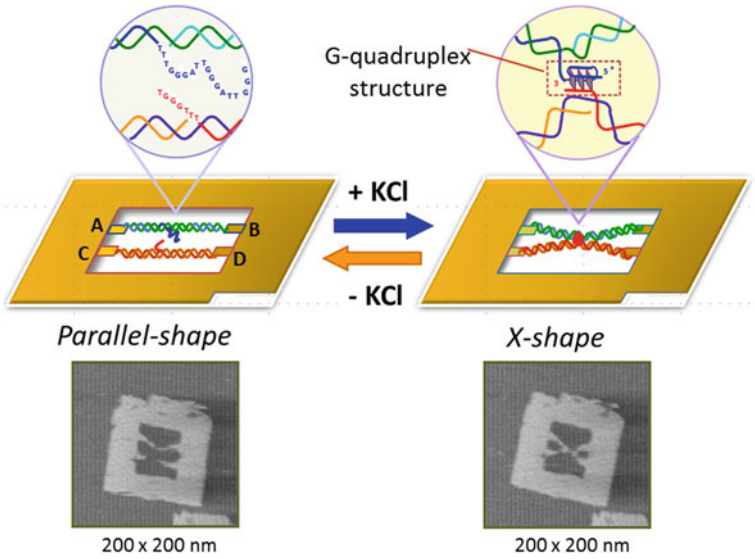

Fig. 1.7 Visualization of the structural changes of two dsDNAs corresponding to the reversible G-quadruplex formation and disruption in the DNA frame. In the presence of KCl, the two dsDNAs were separated. The two dsDNAs formed X-shape at the central positions via G-quadruplex formation by addition of K^+. Reprinted with permission from (Sannohe, Y.; Endo, M.; Katsuda, Y.; Hidaka, K.; Sugiyama, H. *J. Am. Chem. Soc.* **2010**, *132*, 16311–16313). Copyright (2010) American Chemical Society

1.6.3 Single Molecule Fluorescent Imaging

Besides AFM and transmission electron microscopy (TEM), single-molecule fluorescence microscopy also plays an important role particularly for the investigation of complex DNA nanostructures [45]. Taking advantage of the precise addressability of DNA origami each staple strand can be distinguished as a unique attachment point for various nanoobjects such as different fluorophores. Tinnefeld and his coworkers presented a nanoscopic molecular ruler based on DNA origami methods as a general platform for super-resolution microscopy using different imaging techniques [46]. As shown in Fig. 1.8a, a rectangular DNA origami nanostructure containing two fluorescently labeled staple strands at two specific positions (F in black circle), where the distance between them were below the diffraction limit. The assembled structures were immobilized and easily confirmed by AFM. Total internal reflection fluorescence (TIRF) microscopy imaging resulted in a diffraction-limited image in which the emission patterns of two fluorophores were overlapped. However, single fluorophore were identified by using super-resolution fluorescence microscopy (Fig. 1.8a, b). In Fig. 1.8b, the blink microscopy was employed. The fluorescent labeled DNA origami served as rulers

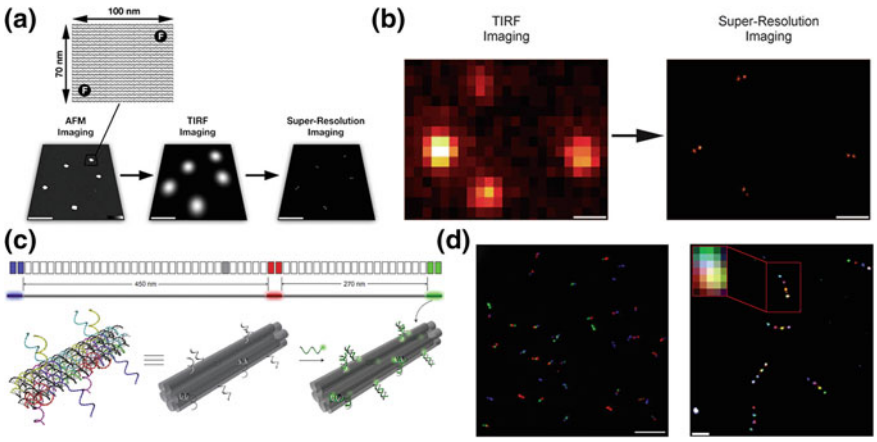

Fig. 1.8 Schematic drawings of DNA molecular nanoscopic ruler. **a** A rectangular DNA origami structures labeled with two fluorophores at two positions below diffraction limit. AFM was used for the confirmation of the nanostructures. TIRF imaging and super-resolution imaging were employed to record the emission patterns of two fluorophores. **b** *Left* TIRF image of surface-immobilized DNA origami labeled with two ATTO655 fluorophores resulting overlapping point-spread functions; *right* super-resolution image of same region using blink microscopy. [DNA Origami as a Nanoscopic Ruler for Super-Resolution Microscopy/Steinhauer, C.; Jungmann, R.; Sobey, T. L.; Simmel, F. C.; Tinnefeld, P./Angew Chemie International Edition, 48/47. Copyright (c) [2009] [copyright owner as specified in the Journal]. **c** Schematics of barcode with a segment diagram on the *top* and a 3D view at the *bottom* and the specific labeled zone in a 3D illustration. **d** *Left* a representative superimposed TIRF image of barcode containing 27 equimolar mixtures of barcode species; *right* a super-resolution fluorescent image of DNA-barcodes. Reprinted by permission from Macmillan Publishers Ltd: [Nature Chemistry] (48), copyright (2012)

for the calibration of super-resolution microscopy and also might be used as quantification standards for other spectroscopic techniques.

A series of geometrically fluorescent barcodes constructed from DNA nanostructures which were assembled with fluorophore-modified DNA strands were developed by Yin and coworkers [47]. A six-helix bundle DNA nanorod was designed and assembled (Fig. 1.8c) where three zones were chosen for the hybridization with three different fluorescent-labeled DNAs, which result the combinations of $3^3 = 27$ barcodes in spatially distribution pattern. After the assembling of DNA nanorods with the specified fluorophores, the barcode system was confirmed by TIRF. A representative image of a pool of all 27 members of barcode family was shown in Fig. 1.8d (left), indicating that the long DNA nanorods exhibited a reliable system to construct geometrically encoded barcodes using fluorescent-imaging technique. By increasing the number of fluorescent zones, the complexity of barcodes can also be enhanced. Meanwhile the resolution

of them can be solved by using super-resolution techniques since the space between neighboring fluorescent zones was under diffraction limit. A super-resolution image of a five-barcode was obtained in Fig. 1.8d (right) using DNA-PAINT [48].

The programmability of DNA origami allows the modification and labeling precisely. Integrating with high spatial resolution technique, DNA origami gradually becomes a powerful method for the single molecule analysis in nanoscale applications.

1.7 Applications to DNA Molecular Machines

DNA based molecular machine is performed by adding extra DNA strand (called "fueling strand") and replacing specific DNA strands containing a "toehold" segment selectively to initiate the mechanical movements in the nanosystem. During the strand displacement, the thermodynamic stabilization energy works for the hybridization of new duplex and control the mechanical movements of DNA machines. By employing this strategy, a DNA based molecular tweezer was created by Yurke and co-workers to perform close-open motions [49]. Another kind of DNA walking device can move autonomously by the cleavage of DNA strand by DNA nicking enzyme [50].

Seeman and coworker developed a rotational mechanical device called "PX-JX2 device", in which the two adjacent ends of dsDNAs can be regulate to rotate in either the PX state and JX2 state by hybridization topology [51–53]. Later two PX-JX2 devices were introduced on the DNA origami scaffold and dynamic patterning were captured on the DNA origami [54]. And a DNA walker was developed to operate the assembly line on DNA origami, in which three PX-JX2 device were also incorporated into the DNA origami framework and then delivered AuNPs to walker which picked up the AuNPs at specific positions [55]. A DNA nanomachine called "DNA spider" were reported by Yan and coworkers [56], in which the programmed operations such as "start", "walk" and "stop" can be incorporated into predesigned track.

A DNA transportation device based on DNA origami was constructed which allow the walking movements along the linear track [57]. A linear track (multiple single stranded DNAs, stators) was introduced to the surface of a 2D DNA tile to guide the stepwise movement of the walking strand (Fig. 1.9a). The cleavage of walker-stator duplex at specific sequence position by nicking enzyme Nt.BbvCI [58] removed a part of stator strands. The walker strand would search for neighboring intact strand and hybridize with it fully by branch migration (Fig. 1.9b). The time-dependent movement of the walker was analyzed by AFM, which was imaged as a single spot representing the walker-stator duplex on the DNA tile. Furthermore, the stepwise movement of the walker was directly observed by high-speed AFM

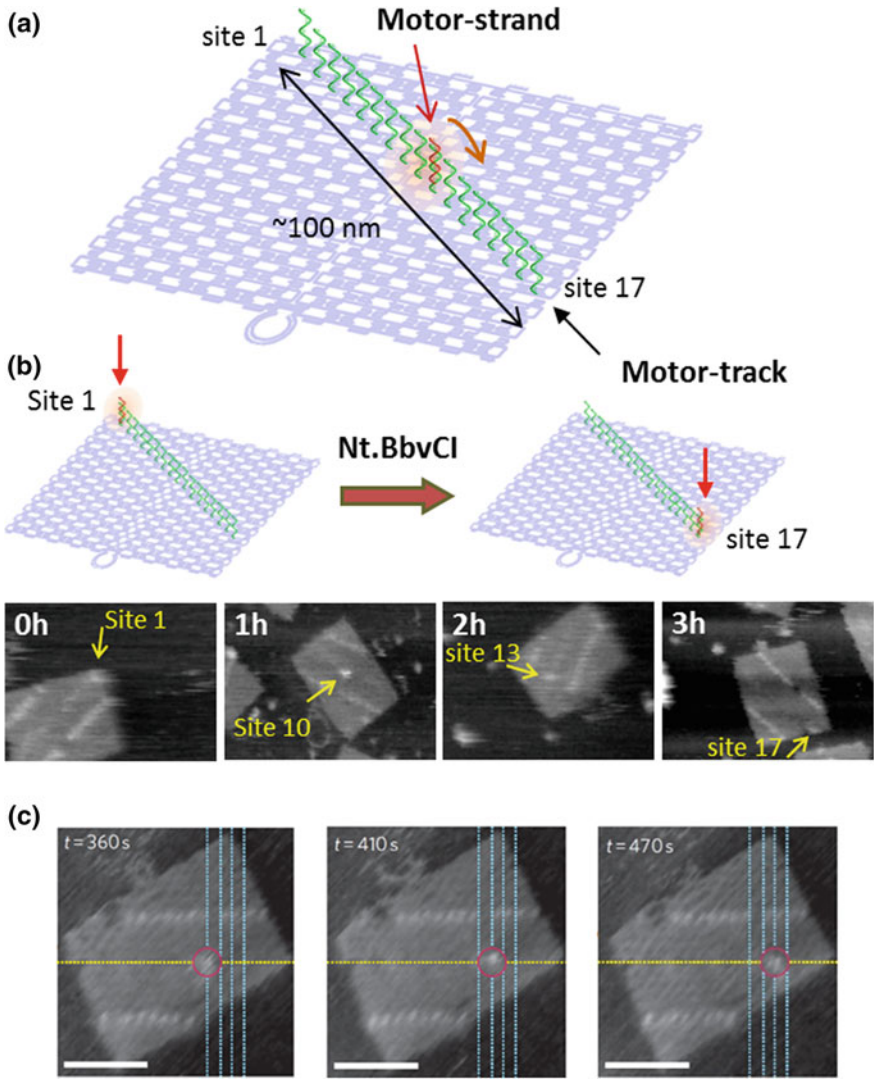

Fig. 1.9 DNA motor on the DNA origami. **a** A 2D DNA tile containing a linear motor track to guide the movement of the motor-strand. **b** Time-dependent movement of a DNA motor by Nt. BbvCI. **c** Step-wise movement of DNA motor observed by high-speed AFM. Scale bar: 50 nm. Reprinted by permission from Macmillan Publishers Ltd: [Nature Nanotechnology] (58), copyright (2011)

(Fig. 1.9c). Our group later designed a complicated walking system for controlling the walking directions using a branched track and controllable blocking strands. The walker's movement along the branched track to defined destination was also directly visualized by high-speed AFM [59]. This method can also be applied to the cargo transportation or perform specific task in limited nanospace.

1.8 Applications to Biological System

The above mentioned various advantages of DNA origami nanostructures have showed great potential for biological applications, which have already been extended to cellular studies. There have been a few examples showing that DNA nanostructures are resistant to various kinds of endo- and exonucleases [60]. Meldrum and co-workers further illustrated that DNA origami constructs could keep integrity without degradation or damage in cell lysate of a series of cell lines [61]. The high stability of DNA nanostructure in biological system and favourable compatibility with functional biomolecules such as proteins and aptamers, demonstrate itself as promising biomaterials for the investigation of living cell analysis and being employed as delivering platforms of safe drug delivery. Unmethylated Cytosine-phosphate-guanine (CpG) oligonucleotides with strong immunostimulatory activities can be recognized by endosomal Toll-like receptor 9 (TLR9) to induce immunostimulatory responses of the immune cells [62, 63]. Fan and co-workers developed a 3D DNA tetrahedra bearing CpG motifs for noninvasive intracellular delivering [64]. And multiple branched DNA nanostructures carrying CpG motifs were developed by Mohri and co-workers for the immune cell deliver [65]. CpG motifs can be accumulated into a hollow tube-shaped origami (Fig. 1.10), which were introduced into the mammalian cells for the investigation of immune responses [66]. The hollow tube containing as many as 62 inner and 62 outter binding sites (Hs) for CpG and anchor sequence was designed in a size of ~80 nm × 20 nm, which is fit with the cellular uptake size. The hollow tube carrying CpG was incubated with isolated mouse splenocyte cells and further fused with a vesicle containing TLR9 segregated by a Golgi apparatus in the endocytic

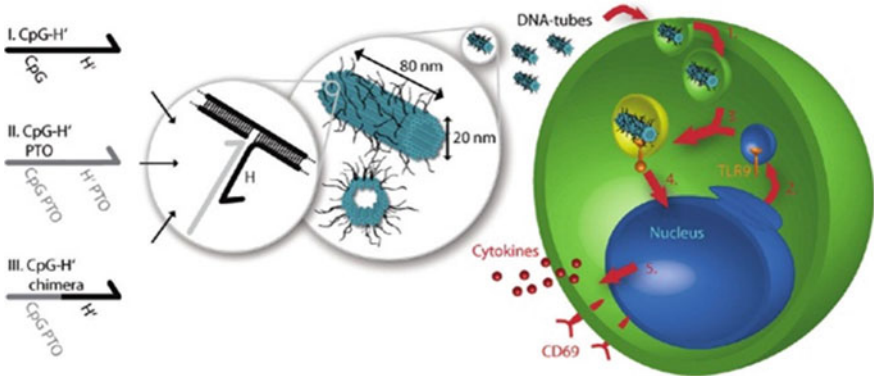

Fig. 1.10 Schematic design of tube-shaped DNA origami and predicted endocytotic pathway. *Left* Three different types of CpG-H'designed to hybridize with CpG. *Right* endocytic pathway of tube origami holding CpG with immune cells and subsequently stimulating the immune responses. Reprinted with permission from (Li, J.; Pei, H.; Zhu, B.; Liang, L.; Wei, M.; He, Y.; Chen, N.; Li, D.; Huang, Q.; Fan, C. *ACS nano* **2011**, *5*, 8783–8789). Copyright (2011) American Chemical Society

pathway. The immune signalling cascade in cell was induced by the recognition of CpG sequences on hollow tube by TLR9. Cytokines and CD69 were further expressed to stimulate the immune response.

Douglas and co-workers designed a 3D hexagonal barrel encapsulated with biomolecules or nanoparticles [67]. The hexagonal barrel was firstly shut by the special DNA latches, which can be unlocked to open by the specific cell-surface proteins (antigen) and the payloads inside will be delivered. The hollow inside can be loaded with different kinds of payloads such as active proteins and nanoparticles. The aptamer locking mechanism can be designed to work in a logic-gated manner according to the different combinations of molecular inputs from target cells. Furthermore, this technique can be used to interface with cells and stimulate the cell signaling responses in an inhibition or activation manner. This programmed DNA-origami based delivery system provides the possibilities of future medical applications such as targeted therapies.

1.9 Conclusion and Prospects

As a bottom-up strategy, DNA origami provides the researchers in nanotechnology a convenient method to realize the construction of nanometer-sized nanostructures in multi-dimensional based on structural DNA nanotechnology. This method affords the possibilities of design and constructs arbitrary nanostructures to satisfy with different purposes. And also this method greatly reduces the experimental labor, eliminates uncertainties to obtain structures in relatively high yield, which greatly increases the efficiency for applications such as single molecule imaging, dynamic mechanical analysis, and cell-targeted delivery and also have already been served for top-down nanotechnology. The constructed nanostructures with pre-designed geometries and specific functionalization exhibit various advantages when compared with other kinds of known biomaterials. As the size of DNA origami is compatible with cellular uptake, the cell-targeted delivery of DNA origami in various shapes with selected functionalization is expected to be applicable. DNA origami can also be employed as assembling components for higher-leveled functionalities with programmed arrangements. The organization and placement of small molecules into confined nanospace is still a challenge. If the preparation of functionalized DNA origami structures can be modified and purified to exclude incomplete portions, the applications of DNA origami method will be greatly improved and become more popular.

DNA origami allows for the addressing functional molecules precisely at pre-determined positions. The nanometer-sized nanostructures are able to accumulate specific synthetic molecules for chemical and biological reactions in nanospace. It is also can be employed as nanoscaffold for the analysis of dynamic molecular behaviors under nanometer resolution in single molecule level. This technology also opens the way to express the complex functionality of the programmed organization of different modules seen in living systems.

References

1. Seeman NC (1982) J Theor Biol 99:237–247
2. Seeman NC (2003) Nature 421:427–431
3. Endo M, Sugiyama H (2009) Chem-Eur J Chem Biol 10:2420–2443
4. Rajendran A, Endo M, Sugiyama H (2012) Angew Chem Int Ed 51:874–890
5. Torring T, Voigt NV, Nangreave J, Yan H, Gothelf KV (2011) Chem Soc Rev 40:5636–5646
6. Rothemund PWK (2006) Nature 440:297–302
7. Högberg B, Liedl T, Shih WM (2009) J Am Chem Soc 131:9154–9155
8. Pound E, Ashton JR, Becerril HcA, Woolley AT (2009) Nano Lett 9:4302–4305
9. Zhao Z, Yan H, Liu Y (2010) Angew Chem Int Ed 49:1414–1417
10. Endo M, Sugita T, Katsuda Y, Hidaka K (2010) Chem–Eur J 16:5362–5368
11. Rajendran A, Endo M, Katsuda Y, Hidaka K, Sugiyama H (2010) ACS Nano 5:665–671
12. Woo S, Rothemund PWK (2011) Nat Chem 3:620–627
13. Zhao Z, Liu Y, Yan H (2011) Nano Lett 11:2997–3002
14. Wei B, Dai M, Yin P (2012) Nature 485:623–626
15. Yin P, Hariadi RF, Sahu S, Choi HMT, Park SH, LaBean TH, Reif JH (2008) Science 321:824–826
16. Douglas SM, Dietz H, Liedl T, Hogberg B, Graf F, Shih WM (2009) Nature 459:414–418
17. Andersen ES, Dong M, Nielsen MM, Jahn K, Subramani R, Mamdouh W, Golas MM, Sander B, Stark H, Oliveira CLP, Pedersen JS, Birkedal V, Besenbacher F, Gothelf KV, Kjems J (2009) Nature 459:73–76
18. Kuzuya A, Komiyama M (2009) Chem Commun 28:4182–4184
19. Ke Y, Sharma J, Liu M, Jahn K, Liu Y, Yan H (2009) Nano Lett 9:2445–2447
20. Endo M, Hidaka K, Kato T, Namba K, Sugiyama H (2009) J Am Chem Soc 131:15570–15571
21. Ke Y, Ong LL, Shih WM, Yin P (2012) Science 338:1177–1183
22. Douglas SM, Marblestone AH, Teerapittayanon S, Vazquez A, Church GM, Shih WM (2009) Nucleic Acids Res 37:5001–5006
23. Chhabra R, Sharma J, Ke Y, Liu Y, Rinker S, Lindsay S, Yan H (2007) J Am Chem Soc 129:10304–10305
24. Shen W, Zhong H, Neff D, Norton ML (2009) J Am Chem Soc 131:6660–6661
25. Rinker S, Ke Y, Liu Y, Chhabra R, Yan H (2008) Nat Nanotechnol 3:418–422
26. Kuzuya A, Kimura M, Numajiri K, Koshi N, Ohnishi T, Okada F, Komiyama M (2009) ChemBioChem 10:1811–1815
27. Saccà B, Meyer R, Erkelenz M, Kiko K, Arndt A, Schroeder H, Rabe KS, Niemeyer CM (2010) Angew Chem Int Ed 49:9378–9383
28. Ke Y, Lindsay S, Chang Y, Liu Y, Yan H (2008) Science 319:180–183
29. Yoshidome T, Endo M, Kashiwazaki G, Hidaka K, Bando T, Sugiyama H (2012) J Am Chem Soc 134:4654–4660
30. Nakata E, Liew FF, Uwatoko C, Kiyonaka S, Mori Y, Katsuda Y, Endo M, Sugiyama H, Morii T (2012) Angew Chem Int Ed 51:2421–2424
31. Voigt NV, Torring T, Rotaru A, Jacobsen MF, Ravnsbaek JB, Subramani R, Mamdouh W, Kjems J, Mokhir A, Besenbacher F, Gothelf KV (2010) Nat Nanotechnol 5:200–203
32. Sharma J, Chhabra R, Andersen CS, Gothelf KV, Yan H, Liu Y (2008) J Am Chem Soc 130:7820–7821
33. Ding B, Deng Z, Yan H, Cabrini S, Zuckermann RN, Bokor J (2010) J Am Chem Soc 132:3248–3249
34. Zhao Z, Jacovetty E, Liu Y, Yang H (2011) Angew Chem Int Ed 50:2041–2044
35. Kuzuya A, Koshi N, Kimura M, Numajiri K, Yamazaki T, Ohnishi T, Okada F, Komiyama M (2010) Small 6:2664–2667
36. Endo M, Yang Y, Emura T, Hidaka K, Sugiyama H (2011) Chem Commun 47:10743–10745

37. Maune HT, Han S-P, Barish RD, Bockrath M, Goddard IIA, RothemundPaul WK, Winfree E (2010) Nat Nanotechnol 5:61–66
38. Youngblood B, Reich NO (2006) J Biol Chem 281:26821–26831
39. Endo M, Katsuda Y, Hidaka K, Sugiyama H (2010) J Am Chem Soc 132:1592–1597
40. Bruner SD, Norman DPG, Verdine GL (2000) Nature 403:859–866
41. Morikawa K, Matsumoto O, Tsujimoto M, Katayanagi K, Ariyoshi M, Doi T, Ikehara M, Inaoka T, Ohtsuka E (1992) Science 256:523–526
42. Endo M, Katsuda Y, Hidaka K, Sugiyama H (2010) Angew Chem Int Ed 49:9412–9416
43. Sannohe Y, Endo M, Katsuda Y, Hidaka K, Sugiyama H (2010) J Am Chem Soc 132:16311–16313
44. Xu Y, Sato H, Sannohe Y, Shinohara K-I, Sugiyama H (2008) J Am Chem Soc 130:16470–16471
45. Birkedal V, Dong M, Golas MM, Sander B, Andersen ES, Gothelf KV, Besenbacher F, Kjems J (2011) Microsc Res Techn 74:688–698
46. Steinhauer C, Jungmann R, Sobey TL, Simmel FC, Tinnefeld P (2009) Angew Chem Int Ed 48:8870–8873
47. Lin C, Jungmann R, Leifer AM, Li C, Levner D, Church GM, Shih WM, Yin P (2012) Nat Chem 4:832–839
48. Jungmann R, Steinhauer C, Scheible M, Kuzyk A, Tinnefeld P, Simmel FC (2010) Nano Lett 10:4756–4761
49. Yurke B, Turberfield AJ, Mills AP, Simmel FC, Neumann JL (2000) Nature 406:605–608
50. Bath J, Turberfield AJ (2007) Nat Nanotechnol 2:275–284
51. Yan H, Zhang X, Shen Z, Seeman NC (2002) Nature 415:62–65
52. Liao S, Seeman NC (2004) Science 306:2072–2074
53. Ding B, Seeman NC (2006) Science 314:1583–1585
54. Gu H, Chao J, Xiao S-J, Seeman NC (2009) Nat Nanotechnol 4:245–248
55. Gu H, Chao J, Xiao S-J, Seeman NC (2010) Nature 465:202–205
56. Lund K, Manzo AJ, Dabby N, Michelotti N, Johnson-Buck A, Nangreave J, Taylor S, Pei R, Stojanovic MN, Walter NG, Winfree E, Yan H (2010) Nature 465:206–210
57. Wickham SFJ, Endo M, Katsuda Y, Hidaka K, Bath J, Sugiyama H, Turberfield AJ (2011) Nat Nanotechnol 6:166–169
58. Bath J, Green SJ, Turberfield AJ (2005) Angew Chem Int Ed 44:4358–4361
59. Wickham SFJ, Bath J, Katsuda Y, Endo M, Hidaka K, Sugiyama H, Turberfield AJ (2012) Nat Nanotechnol 7:169–173
60. Castro CE, Kilchherr F, Kim D-N, Shiao EL, Wauer T, Wortmann P, Bathe M, Dietz H (2011) Nat Meth 8:221–229
61. Mei Q, Wei X, Su F, Liu Y, Youngbull C, Johnson R, Lindsay S, Yan H, Meldrum D (2011) Nano Lett 11:1477–1482
62. Vollmer J, Krieg AM (2009) Adv Drug Delivery Rev 61:195–204
63. Latz E, Verma A, Visintin A, Gong M, Sirois CM, Klein DCG, Monks BG, McKnight CJ, Lamphier MS, Duprex WP, Espevik T, Golenbock DT (2007) Nat Immunol 8:772–779
64. Li J, Pei H, Zhu B, Liang L, Wei M, He Y, Chen N, Li D, Huang Q, Fan C (2011) ACS Nano 5:8783–8789
65. Mohri K, Nishikawa M, Takahashi N, Shiomi T, Matsuoka N, Ogawa K, Endo M, Hidaka K, Sugiyama H, Takahashi Y, Takakura Y (2012) ACS Nano 6:5931–5940
66. Schüller VJ, Heidegger S, Sandholzer N, Nickels PC, Suhartha NA, Endres S, Bourquin C, Liedl T (2011) ACS Nano 5:9696–9702
67. Douglas SM, Bachelet I, Church GM (2012) Science 335:831–834